

CRACK PATH INSTABILITY IN ALUMINIUM LITHIUM ALLOYS

Y. H. Tai, D. T. Asquith and J. R. Yates

Dept of Mechanical Engineering, University of Sheffield, UK.
E-mail: y.tai@sheffield.ac.uk

ABSTRACT. *Anisotropy and crack path stability in aluminium lithium alloys remain a concern which has limited its widespread use especially in primary structural components. The aim of this work is to investigate the crack path stability of 2050-T851 aluminium lithium alloy in ductile tearing of compact tension specimens loaded under quasi-static mode I conditions. Results show significant anisotropy exists in 2050-T851 but it has been significantly improved when compared to previous results obtained for 2195. Initial analysis of the fracture surfaces and experimental data has produced some interesting observations which warrant further investigation into the role of microstructure.*

INTRODUCTION

There are numerous benefits of using modern aluminium lithium alloys for applications where weight is of importance because of the reduced strength, increased strength and elastic modulus. However, due to the alloying and thermomechanical processing and hence resultant microstructure, these alloys tend to possess significant anisotropy in both mechanical properties and fracture behaviour. The latest generation of aluminium lithium alloys have been improved significantly but do still suffer from these problems which have limited their widespread use.

The aim of this paper is report on preliminary findings from tear tests conducted on a fourth generation aluminium lithium alloy designated 2050-T851. The results obtained will be compared with results obtained from experiments carried out using a previous generation alloy designated 2195 [1]. 3D digital image correlation (DIC) was used as the primary method of data acquisition and analysis. It is anticipated that the full field measurements would allow for the out of plane deformation to be quantified and related to the plastic zone size. Following this section will be a brief explanation of the principles behind DIC. Subsequently, the experimental work undertaken will be detailed which will then followed by the preliminary results obtained. Finally appropriate conclusions will be drawn.

BASIC PRINCIPLES OF DIGITAL IMAGE CORRELATION

A digital image is essentially a two-dimensional array of intensity values which can be divided further into small subsets. 2D image correlation works by matching small square subsets of an undeformed image to locations in the image of the surface after deformation (as illustrated in Figure 1) by means of mapping and cross correlation functions. Further information regarding the functions and technique used can be found here [2].

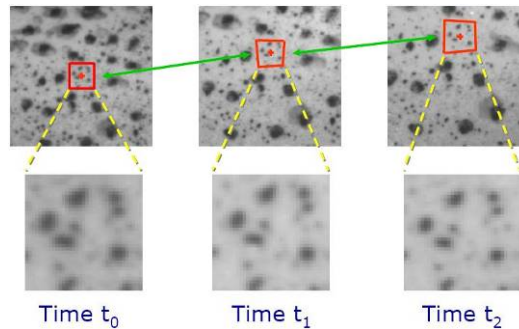


Figure 1: Illustration of subset matching and deformation tracking used for DIC (*Image courtesy of Limes GmbH*)

In this work a 3D DIC system, Vic3D provided by Limes GmbH was used. 3D DIC is more complicated but it basically uses a projection and back projection technique to achieve the 3D full field displacement measurements. This technique is claimed to eliminate perspective distortion of the lenses and inherent uncertainty in triangulation methods. Further information can be found here [3].

EXPERIMENTAL WORK

Material

The material used in this work was an aluminium lithium alloy designated 2050-T851 which was provided by Airbus UK in 15 mm thick plate form. The composition specifications provided can be seen in Table 1. It has low lithium content but this is a common feature of modern aluminium lithium alloys due to the detrimental effects of lithium precipitates [4].

Table 1: Chemical composition of 2050-T851 (wt%)

| Ag | Zr | Mn | Cu | Si | Mg | Li | Zn | Al |
|------|------|------|------|------|------|------|------|---------|
| 0.36 | 0.09 | 0.38 | 3.51 | 0.03 | 0.40 | 0.91 | 0.02 | Balance |

Tensile test

Standard tensile tests were performed to obtain the material stress strain curve. As the material was supplied in 15 mm plate form, the tensile specimens could be machined into round cross-section with a diameter in the gauge length of 8.0 mm. The specimens were cut from both L (loading along rolling direction) and T directions (perpendicular to rolling direction) to determine the extent of material anisotropy. A random speckle pattern was applied to the surface to facilitate the displacements measurements using DIC. Figure 2 shows one of the prepared specimens.



Figure 2: Prepared tensile specimen with speckle pattern on surface

The tensile tests were in a 100kN servo electric Mates test machine in displacement control mode at a rate of 0.01 mm/s. 2D DIC was used to measure the elongation of the specimen. To minimise problems caused by paint crazing, the surface was sprayed lightly with a combination of black and white acrylic based spray paint. This gave a good random speckle pattern which can be seen in Figure 2. In order to minimise problem caused by reflections from the surface of the specimen especially when out of plane deformation occurs, photographic dulling spray was applied prior to testing. Figure 3 shows the experimental set used for this work. A total of four tests were done, two in each direction.



Figure 3: Tensile test experimental set-up with 2D DIC

Tear test

For crack path instability and tearing toughness tests, thin sheet CT specimens were machined from the plate into 10 mm thick specimens. The design of the specimen was based on the guidelines in the ASTM E2472 standard [5] and had in-plane dimensions of 100 x 96 mm. The specimens were machined from the plate in both TL (crack propagating along rolling direction) and LT (crack propagating across to rolling direction) configuration. The notch was machined by electrode discharge machining (EDM). The specimens were fatigue pre-cracked prior to testing to generate a sharp crack in a bid to minimise crack path instability at initiation.

Fatigue pre-cracking was done at a $\Delta K_I = 24 \text{ MPa}\sqrt{\text{m}}$ which is approximate 60 percent of the fracture toughness of this material at a R ratio of 0.1. It required approximately 5000 cycles to generate fatigue cracks $\sim 1 \text{ mm}$ long which results in a final notch length of 36 mm and crack length to specimen width ratio of 0.45. This will allow for approximately 25 mm of geometry independent crack extension. Figure 4 below is a schematic diagram of the CT specimen used in this study.

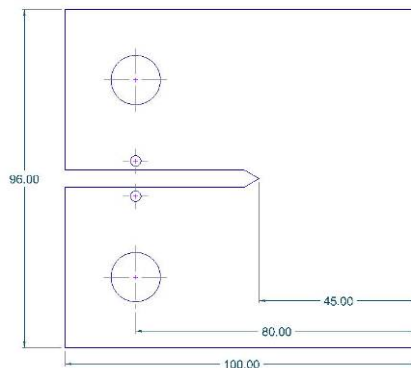


Figure 4: Schematic of 10 mm thin sheet CT specimen

The tests were carried in a servo hydraulic Mayes test frame with hydraulic grips. Bespoke grips were made to hold the specimen and minimise buckling during the tearing process. Displacement rate of the actuator was set at 0.05 mm/s which meant the tests were carried out under quasi-static conditions. 3D DIC was intended to be used for displacement measurements which required a random speckle pattern to be applied on the surface of the specimens. This was done by spraying the area of interest with white paint which was then speckled using black paint. Figure 5 below shows a prepared specimen loaded in the grips prior to tearing. Image acquisition and data acquisition was done with the Vic3D DIC system which allowed for the synchronisation of parameters of interest (eg. load and actuator displacement) with the images obtained.

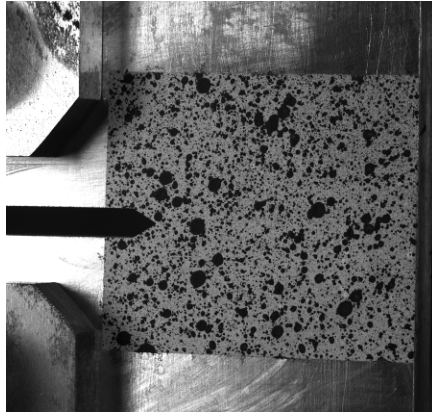


Figure 5: Prepared CT specimen loaded in grips prior to testing

RESULTS AND DISCUSSION

Results from the tensile test show that this material exhibits a small degree of anisotropy in its behaviour as illustrated by Figure 6 below. The mechanical properties obtained from the experimental data are summarised in Table 2. Total elongation of specimens in both directions was quite similar at 7.5% and 7.8%. However, the strain hardening behaviour differs slightly. Ultimate tensile strength in the L direction occurs at 4.2% strain where as the ultimate tensile strength in the T direction occurs when strain levels reached 5.8%.

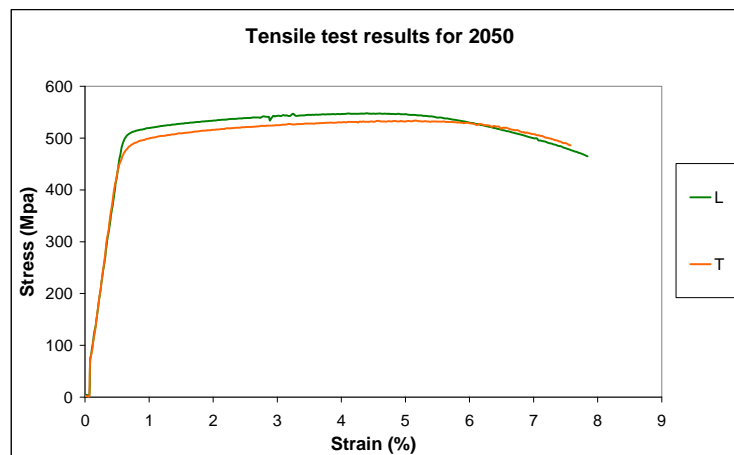


Figure 6: Stress strain curves for 2050 in L and T direction

Table 2: Mechanical properties obtained from tensile tests

| Direction | Yield Strength 0.2%(MPa) | Tensile Strength (MPa) | Elongation (%) |
|-----------|--------------------------|------------------------|----------------|
| L | 500 | 545 | 7.8 |
| T | 470 | 528 | 7.5 |

From the tensile test results, there was a good indication that anisotropic behaviour will be observed in the tear tests. However, the extent of the anisotropy was not expected. Figure 7 shows the torn specimens with out of plane deformation maps superimposed on the surface. The crack path of the specimen in the LT direction is highly unstable. There was a significant amount of crack tunnelling and the fracture mode comprised of a combination of slant and shear fracture.

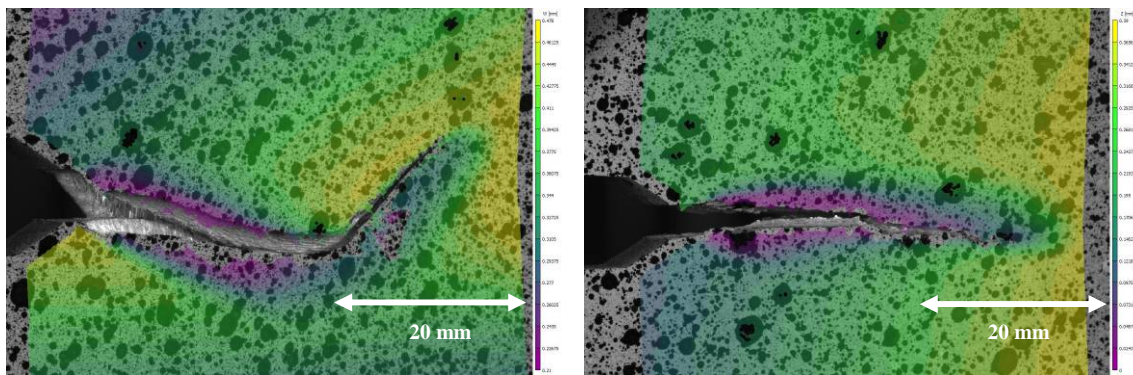


Figure 7: Out of plane deformation maps of tear specimens, LT (left) and TL (right)

Further evidence of the fracture instability is encountered in the load CMOD plot for the LT specimen shown in Figure 8. There is a sudden drop in load (21 kN to 7.2 kN) which in turn was followed by the crack beginning to turn approximate 45 degrees as shown in Figure 7. The corresponding CMOD increases by 0.37 mm (1.16 mm to 1.53 mm). Preliminary investigation of the fracture surface suggests sudden fracture between grain boundaries to be the most likely cause. The cause of the crack turning has not been established but based on literature data it would most likely be microstructure related [4]. Further analysis of the fracture surfaces and data is needed to determine the cause of this phenomenon.

For the specimen in the TL direction, the crack path was deemed to be stable. There was minimal amount of crack tunnelling and it was predominantly flat fracture throughout the tearing process with only small shear lips forming at the edges. The tearing resistance was significantly less when compared to the LT direction. Comparing results from the tensile test and tear test, it is clear that the difference in anisotropy is significantly greater for the tear test.

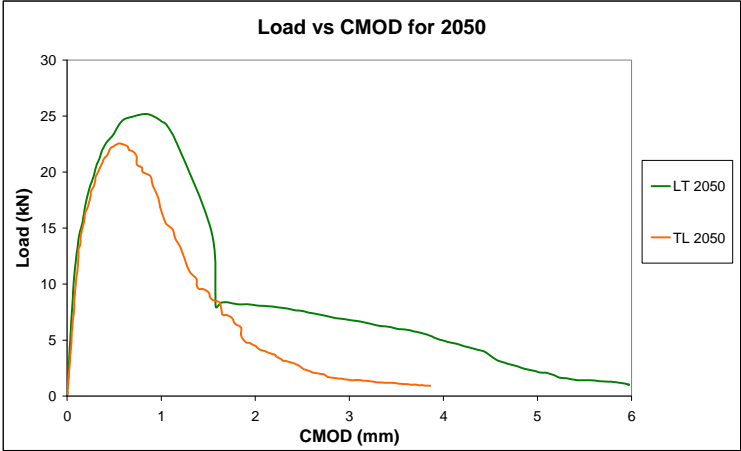


Figure 8: Load CMOD for 2050 CT tear specimens

If the results are compared to previous results obtained from similar experiments using 2195 [1], it can be shown that there is an improvement in the tearing properties of 2050. Figure 9 shows the torn 2195 specimens. The difference in tearing toughness between TL and LT is significant greater as illustrated in Figure 10. Severe crack tunnelling was observed in the LT direction and there were periodic sudden drops in load during the fracture process which was followed by deviation in the crack path as shown in Figure 9.

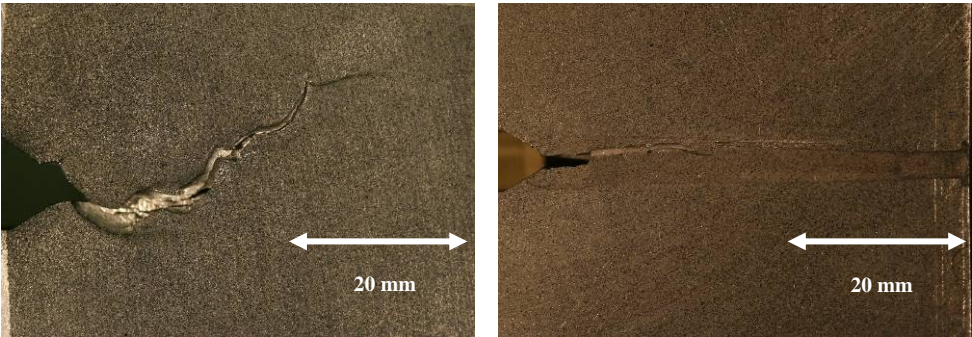


Figure 9: Torn 2195 specimens, LT (left) and TL (right)

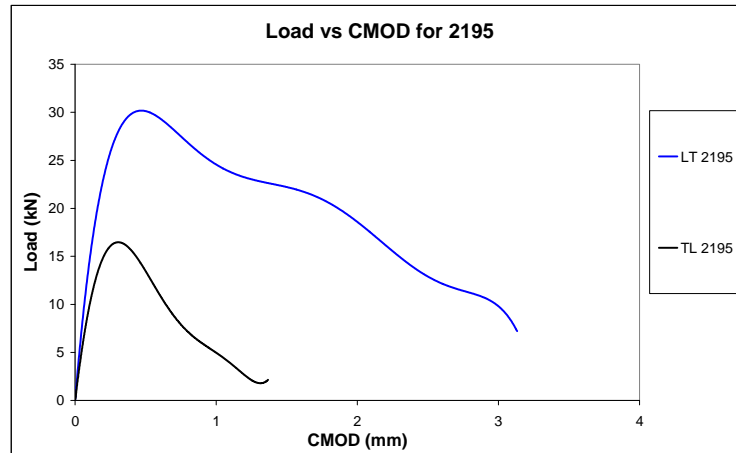


Figure 10: Load CMOD for 2195 CT tear specimens

CONCLUSIONS AND FUTURE WORK

Preliminary investigation into the anisotropic behaviour of 2050-T851 has shown this material to have improved tearing properties compared to 2195. However, crack path instability in the LT direction for both alloys is an issue which warrants further investigation. The sudden drop in load leading to a deviation in crack path is another interesting feature worth looking into. Work is currently underway to develop methods of extracting useful fracture data from the 3D displacement fields which would help to better quantify and understand the causes of the anisotropy. An investigation into the distinctly different fracture surfaces observed would also determine the role material microstructure.

REFERENCES

1. Tai Y H, Asquith D T, Pinna C, and Yates J R. in *ECF 17*. 2008. Brno, Czech Republic.
2. Sutton M A, Cheng M, Peters W H, Chao Y J, and Mcneil S R, 1986 *Image and Vision Computing*. **4**(3): p. 143-150.
3. Limes. *Vic3D Manual*.
4. Martins J W, 1988 *Annual Review of Material Science*. **18**: p. 101-119.
5. ASTM-E2472 (2006).